Journal of Applied Polymer Science

Biocomposites based on chemically modified cellulose fibers with renewable fatty-acid-based thermoplastic systems: Effect of different fiber treatments

M. Reulier,[1] R. Perrin,[2] L. Avérous[1]

[1]BioTeam/ICPEES-ECPM, UMR CNRS 7515, Université De Strasbourg, 25 Rue Becquerel, Strasbourg Cedex 2, 67087, France

[2]SOPREMA, 14 Rue De Saint Nazaire, CS 60121, Strasbourg Cedex, 67025, France

Correspondence to: L. Averous (E-mail: luc.averous@unistra.fr)

ABSTRACT: Advanced biocomposites, based on binary and ternary systems, were developed with thermoplastic matrices such as thermoplastic polyurethane (TPU) and polyamide (DAPA) obtained from dimers of fatty acids, and cellulose fibers (CF). The CF were modified to display high interfacial adhesion and compatibility with the rather hydrophobic matrices. Different routes were considered such as grafting onto with prepolymers, or grafting from with aromatic isocyanate or fatty acid. An original approach of this work is to consider CF as a polyol with an equivalent hydroxyl index obtained by titration. In order to understand better the effect of each phase, the resulting modified CF were tested with neat TPU and DAPA matrices. The most promising fibers treatments were then tested with 80/20 and 50/50 wt %/wt % TPU/DAPA blends. Properties at the molecular and macromolecular scale were investigated. Improvement of the interfacial adhesion between the fibers and the polymers were observed. From the different grafting approaches tested, the best performing were the isocyanate-terminated prepolymer and the silane-terminated prepolymer modifications. In comparison with neat CF, modification with isocyanate-terminated prepolymer improved threefold the storage and Young's modulus of TPU biocomposites. © 2016 Wiley Periodicals, Inc. J. Appl. Polym. Sci. **2016**, *133*, 43878.

KEYWORDS: biopolymers & renewable polymers; composites; fibers; polyamides; polyurethanes

Received 8 January 2016; accepted 29 April 2016

DOI: 10.1002/app.43878

INTRODUCTION

Over the last decades, the production of renewable materials as an alternative to petroleum-based materials has attracted considerable attention from both academic and industrial groups. From these renewable materials, multiphase systems with advanced behaviors can be developed such as the biocomposites where both, matrices and fillers are bio-based.[1–3] Recent studies carried out by our group on thermoplastic polymers synthesized from dimers of fatty acid (DFA), such as polyurethane (TPU) and polyamide (DAPA), has shown the great advantage of TPU-DAPA blending,[4,5] since TPU and DAPA present two distinct behaviors. TPU is a thermoplastic elastomer and DAPA exhibits the behavior of a typical semi-crystalline thermoplastic. Dimer fatty acid-based blends (TPU/DAPA), due to the associated singular macromolecular structures show relatively good performances, for instance DAPA improves Young's modulus and tensile strength at break of the TPU phase.[4] Recently we showed that a method of improving the mechanical properties of these multiphase systems is to develop composites, with mineral micro-fillers.[5] However, this route presents some drawbacks such as weak matrix/filler interfaces, and a lower renewable content. For this reason another approach was necessary, taking into consideration bio-based reinforcing materials such as (ligno-)cellulose fibers.[2,3,6–9]

It is very well-known that cellulose fibers (CF) have many attractive properties including low density, high stiffness, ability to recycle, and widespread availability at a rather low cost,[10] which motivates more and more industrial sectors (e.g., automotive, building) to replace common synthetic or glass fibers. However, the main disadvantage of CF, and bio-based fibers in general seems to be the highly polar and hydrophilic character that is associated with a weak interfacial compatibility with hydrophobic thermoplastic matrices. This latter factor can limit the fibers dispersion in the melted matrix and can contribute to poor stress transfer between the components under manipulation. To overcome this issue, in recent decades, researchers have focused their attention on finding suitable modifications in the area of CF-reinforced thermoplastic composites. Different

Additional Supporting Information may be found in the online version of this article.

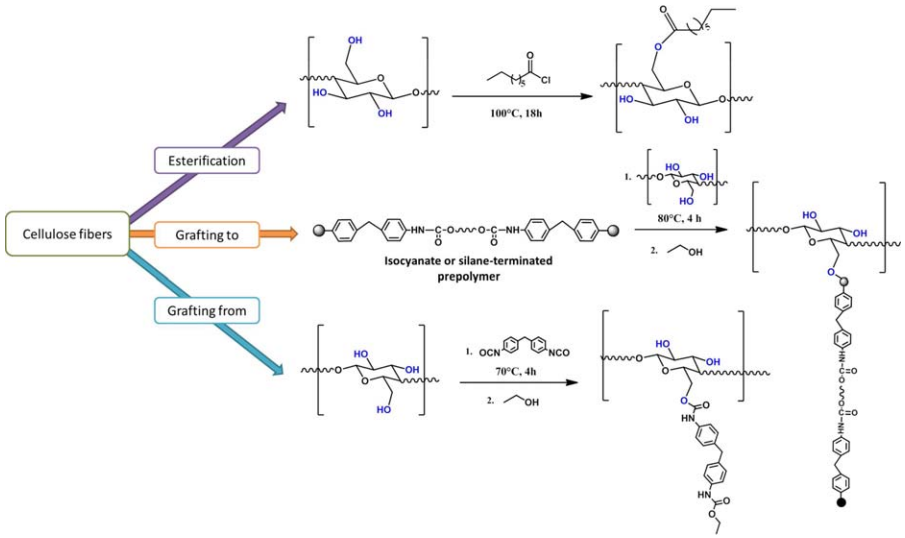

Figure 1. Illustration of the different modifications of the cellulose fibers. [Color figure can be viewed in the online issue, which is available at wileyonlinelibrary.com.]

chemical modifications such as esterification with fatty acids, silane treatments, acetylation, mercerization, isocyanate treatments, or graft copolymerization of methyl methacrylate are most commonly reported.[6,11–18] Modifications are based generally on the use of reagents with functional groups, which principally react with the free hydroxyl functions (OH) at the surface of the CF.

The aim of this work was to develop different advanced biocomposites, associating modified CF with different matrices such as DAPA, TPU, or the corresponding TPU/DAPA blends in connection with previous recent studies.[4,5] Chemical modifications of the fibers is always carried out considering a certain percentage of the OH groups on the CF. Therefore, the first original approach of this work was to consider CF as a polyol, with an equivalent hydroxyl index (I_{OH}) obtained by titration. Neat CF were functionalized either to introduce them into a DAPA or a TPU phase. After some preliminary tests, three different pathways were chosen to modify the fibers. They are illustrated in Figure 1. These grafting approaches were carried out to modify the hydrophobic/hydrophilic balance of the fibers, decreasing the hydrophilic character of the cellulose at the surface. The esterification is expected to decrease the fibers-fiber interactions reducing their tendency to aggregate and to decrease their moisture sensitivity. The two other modifications were expected to promote hydrogen bonding with the polar groups of the matrices in order to increase the matrix-fibers interactions at the interface. The long grafted chains used may also improve the stress transfer by interdiffusion with the matrix. To compare the efficiency of these fibers treatments, different analyses such as FTIR or I_{OH} titration were used. The most promising modified fibers were then introduced in TPU/DAPA blends to obtained ternary biocomposites.

EXPERIMENTAL

Materials

Neat CF (Arbocell) with an average length and thickness of 300 and 20 μm, respectively, obtained from leafwood with a purity of 99.5% were provided by J. Rettenmaier & Söhne (Germany). Radiacid 0608, principally based on octanoic acid (OA) (99.2% C8) a transparent yellow liquid with an acid number of 387 mg KOH g^{-1}, and polyester polyol (D_{3000}), based on dimeric fatty acids from rapeseed oil with a hydroxyl value of 33 mg KOH g^{-1}, and a molar mass of 3000 g mol^{-1} were kindly supplied by Oleon (France). An amorphous polyester polyol (D_{2000}) based on dimeric fatty acid from rapeseed oil, with a hydroxyl value of 52 mg KOH g^{-1} and a molar mass of 2000 g mol^{-1} was provided by Croda (United Kingdom). Polyether monol (M_{700}) based on lauric acid, with a hydroxyl value of 79 mg KOH g^{-1} and a molar mass of 700 g mol^{-1}, was provided by Repsol (Spain). *N*-(*n*-butyl)−3-aminopropyl-trimethoxysilane was supplied from Evonik (Germany). A di-functional uretonimine modified 4-4′-diphenylmethane diisocyanate (MMDI) (NCO content of 30.9%) and 4-4′-diphenylmethane diisocyanate (MDI) (NCO content of 33.5%) were purchased from Huntsman (United States).

DAPA was provided by Arkema (France), under the trade name of Platamid HX. DAPA is a semi-crystalline polymer with a glass transition (T_g) at 6 °C and a melting temperature (T_m) of 120 °C. TPU was prepared with an isocyanate/hydroxyl (NCO:OH) ratio equal to 1 and a hard segments (HS) content of 17 wt % using a two-step process. During the first step, a prepolymer with NCO end groups is obtained. In a second step, the high molar mass TPU is prepared with 1,4-butanediol (BDO) as a chain extender. The detailed synthesis has been fully described in a previous publication.[19] The corresponding TPU showed a glass transition of −48 °C, which is related to the presence of soft segments (SS).

BDO, thionyl chloride (TC), phthalic anhydride, hydrochloric acid, ethyl acetate, diethyl ether, ethanol, isopropanol, and 2-butanone with purities of 99.0% were all purchased from Sigma Aldrich (France). Pyridine was purchased from Fischer Scientific (France). These chemicals were used without any further purification.

Table I. SEC Analyses Results with Molar Masses and Dispersity Values

	P_{700}	P_{2000}	P_{3000}	S
M_w (g mol^{-1})	3 400	23 570	36 890	23 900
M_n (g mol^{-1})	2 260	10 750	16 780	11 810
$Đ = M_w/M_n$	1.5	2.2	2.2	2.0

Modification of CF

Three different grafting methods were investigated (Figure 1). The hydroxyl index (I_{OH}) was measured and reported in Table II, before and after the CF modifications.

Esterification of CF. Esterification of the surface of the CF was performed with OA. In order to improve the reactivity of OA, a chlorination step was first carried out. According to the procedure described by Thiebaud *et al.*,[20,21] the esterification was performed without solvent and catalyst using TC. The chlorination step was carried out in a three-necked 500 mL round-bottomed flask equipped with a magnetic stirrer.[22] A nitrogen-gas bubbling system connected to a wash-bottle containing oil was used to trap any hydrogen chloride evolved. The chlorination step was performed with an excess of TC, where OA:TC ratio was 1:2. OA (25 g, 0.173 mol) was first dissolved in ethyl acetate (200 mL) and then cooled to 0 °C under a nitrogen flow. TC (41.26 g, 0.346 mol) was then added dropwise at 0 °C and the reaction mixture was finally heated at 60 °C for 8 h. The solvent and the excess of TC were then distilled off under rotary evaporation. Octanoyl chloride (OC) was obtained as a brown liquid. NMR and IR analyses of OC are reported in the Supporting Information (Figures SI-1 and SI-2).

The esterification procedure was performed in a 100 mL reactor with a mechanical stirrer and a nitrogen-gas bubbling system connected to a wash-bottle was used to trap any hydrogen chloride formed. Dried CF (5.04 g, 27 mmol OH) and OC (32.12 g, 198 mmol) were successively introduced in the reactor. The reaction was then conducted at 100 °C under a continuous nitrogen stream with constant stirring for 18 h. At the end of the reaction, yellowish fibers were obtained. Esterified cellulose fibers (ECFs) were first washed with diethyl ether and then with ethanol using a soxhlet extraction. Finally, ECFs were dried overnight at 70 °C under vacuum.

Grafting from via an Isocyanate Route. In a 100 mL reactor equipped with a mechanical stirrer under inert atmosphere, dried CF (13 g, 71 mmol OH) and MMDI (70.2 g, 516 mmol NCO) were introduced. The reaction shown in Figure 1 was carried out for 4 h at 70 °C. The isocyanate-modified cellulose fibers (ICF) were then filtered and washed with ethanol (500 mL) to form urethane groups with the unreacted isocyanate. The compound was then dried overnight at 70 °C under vacuum.

Grafting onto via Different Prepolymers Routes. CF was then modified via a grafting to approach with polyurethanes-based prepolymers and different end groups (Figure 1)

Isocyanate-Terminated Prepolymers Synthesis. Three isocyanate prepolymers were first synthesized with different molar masses and with a constant NCO:OH molar ratio, using a monol (M_{700}) or two different diols (D_{2000} and D_{3000}). The monol or polyol and MMDI ($f = 2$) were added under inert atmosphere in a three-necked 500 mL round-bottomed reactor equipped with a mechanical stirrer. The NCO:OH molar ratio was 2:1, and the mixture was stirred at 70 °C. The kinetics of the reaction were followed by NCO titration. The reaction was stopped once the theoretical NCO concentration was reached. The ensuing isocyanate prepolymers were coded as P_{700}, P_{2000}, and P_{3000} for syntheses with monol or diols with molar masses of 700, 2000, and 3000 g mol^{-1}, respectively. Molar masses obtained by size exclusion chromatography (SEC) are reported in Table I.

Silane-terminated prepolymer synthesis. P_{2000} (252.3 g, 196 mmol) and *N*-(*n*-Butyl)−3-aminopropyl-trimethoxysilane (46.6 g, 196 mmol) were introduced into a 100 mL three-necked reactor to obtain a silane-terminated prepolymer (coded as S). The system was stirred at 60 °C and the reaction was stopped when the free-isocyanate concentration reached zero. Molar masses obtained by SEC are reported in Table I.

Synthesis of the modified CF. All chemical modifications were carried out in a 100-mL three-necked reactor under reflux in an inert atmosphere.

CF grafting (38.8 g, 0.21 mol) with the silane-terminated prepolymer (50 g, 0.21 mol) was carried out with 50 mL of 2-butanone. The temperature was set to 70 °C and the reaction was stirred for 4 h. On completion, the fibers were washed with THF. Finally, these modified CFs (coded as SCF) were dried overnight at 70 °C, under vacuum.

Fifty milliliters of 2-butanone was also added in the case of the grafting based on P_{3000}, to reduce the high viscosity of the reaction mixture. All other reactions were performed without solvent. A NCO:OH molar ratio of 1:1 was used for each reaction and calculated using the hydroxyl index of the CFs and the NCO content of the prepolymers. The reaction was stirred at 80 °C for 4 h. Once complete, the fibers were washed with ethanol to remove any unreacted isocyanate and then with THF. The modified CFs were finally dried overnight at 70 °C under vacuum. The resulting modified CFs were coded as P_{700}CF, P_{2000}CF, or P_{3000}CF with the prepolymers P_{700}, P_{2000}, or P_{3000}, respectively. To simplify reading, P_{xxx}CF code will be used to regroup P_{700}CF, P_{2000}CF, and P_{3000}CF.

Preparation of the Biocomposites

Prior to the melt-mixing, the TPU, DAPA pellets, and fibers were dried overnight at 70 °C under vacuum. The biocomposites were prepared using an internal mixer (counter-rotating mixer Rheomix 600p, Haake) equipped with a pair of high-shear roller-type rotors at 150 °C with a speed of 80 rpm for 8 min. After melt processing, the materials were compression-molded to obtain sheets with a hot press at 160 °C applying a pressure of 160 bars for 5 min. The sheets were further squeezed and cooled down at room temperature between two steel plates for 5 min. Grafted fibers were introduced at a weight ratio of 10 wt % into the thermoplastic matrix, considering the cellulose content.

The weight ratios (wt %/wt %) of the TPU/DAPA blend systems were 80/20 and 50/50. The corresponding biocomposites are designated as follows: TPU/DAPA (X/Y)_fiber 10, where X/Y is equal to the TPU/DAPA weight ratio, with $X+Y=100$. As an example, "TPU/DAPA (80/20)_CF 10" or "(80/20)_CF 10" correspond to a biocomposite where the weight ratio of the TPU/DAPA system is 80/20 (wt %/wt %) and the CF content is of 10 wt %.

General Methods

Infrared spectroscopy was achieved with a Fourier transformed infrared spectrometer Nicolet 380 (Thermo Electron Corporation), working in reflection mode and equipped with an ATR diamond module (FTIR-ATR). The FTIR-ATR spectra were collected in the range of 4000 and 400 cm^{-1} with an accumulation of 16 scans.

The number-average molar mass (M_n), the mass-average molar mass (M_w), and the dispersity ($Đ$) of the prepolymers were determined by SEC, using a Malvern Instrument apparatus (Viscotek RImax). This device was equipped with a 10 mm guard column (8 µm) and three 300 mm columns (50, 150, and 500 Å). Refractive index (RI) and ultraviolet (UV) detectors were used. Tetrahydrofuran (THF) was used as an eluent with a flow rate of 1 mL min^{-1}. Linear polystyrene from 162 to 20,000 g mol^{-1} was used to calibrate the apparatus.

The degree of substitution (DS) of the modified CF was determined by elemental analysis using a ThermoFisher Scientific "Flash 2000." Each sample was analyzed in duplicate with an absolute precision of 0.3%.

The hydroxyl index (I_{OH}) is a key parameter in the characterization of polyols. This value is the number of milligrams of KOH equivalent to the OH content of 1 g of polyol. I_{OH} was determined by the standard esterification method using phthalic anhydride.[23] Polyol (1 g) and a 1.0 M solution of phthalic anhydride in pyridine (20 mL) were heated at 130 °C for 45 min and cooled to room temperature. Pyridine (30 mL) was added and then water (30 mL). The solution was then titrated with a 1.0 M sodium hydroxide (NaOH) solution. I_{OH} in mg of KOH g^{-1} was determined according to eq. (1).

$$I_{OH}=\frac{(V_{blank}-V_s)\times C\ \times 56.1}{W_s} \quad (1)$$

where V_{blank} (mL) and V_s (mL) are the volumes of NaOH solution required for blank and polyol sample titrations, respectively. C (mol L^{-1}) is the concentration of the NaOH solution and W_s (g) is the polyol weight.

%NCO was determined by indirect titration of an excess of dibutylamine by HCl solution. In a beaker, isocyanate (1 g) and a 1.0 M solution of dibutylamine (25 mL) were mixed. The beaker was closed and stirred during 10 min at room temperature. Isopropanol (50 mL) was then added. Finally, the solution was titrated with a 1.0 M hydrochloric acid (HCl) solution. A blank sample (without any isocyanate) was also titrated in order to determine the total quantity of dibutylamine introduced. %NCO was determined according to eq. (2).

$$\%NCO=\frac{(V_{blank}-V_s)\times C\ \times 4.2}{W_s} \quad (2)$$

where V_{blank} (mL) and V_s (mL) are the volumes of HCl solution required for the blank and the isocyanate sample titrations, respectively. C (mol L^{-1}) is the concentration of the HCl solution and W_s (g) is the isocyanate weight.

Contact angles were determined using the sessile drop method on a GBX Digidrop R&D LC goniometer (France) equipped with a video camera. To obtain homogenous surfaces, fibers were compression-molded at room temperature under a 160 bars pressure for 2 min. A droplet of water was deposited onto the surface of the sample and the evolution of the contact angle was followed for 10 minutes.

Thermogravimetric analyses (TGA) of fibers, polymer blends, and composites were performed on a Hi-Res TGA 2950 apparatus from TA Instruments. Samples were heated from room temperature up to 700 °C at a rate of 20 °C min^{-1} under air flow. The temperature at the maximum of the derivative thermogram curve (T_{DTGmax}), the $T_{98\%}$ temperature, and the $T_{2\%}$ temperature where the sample weight is respectively equal to 98% and 2% were reported.

Thermal characterization was performed using a TA Instruments Q 200 under nitrogen (with a flow rate of 50 mL min^{-1}). All samples were weighted between 2 and 5 mg. The samples were heated up to 160 °C with a heating rate of 10 °C min^{-1} (first heating scan), then cooled down to −80 °C at 10 °C min^{-1} and finally re-heated to 160 °C at a heating rate of 10 °C min^{-1} (second heating scan). In these temperature ranges, we can show by thermo-gravimetric analysis that the thermal degradation of the corresponding matrixes do not occur. The glass transition (T_g) and the melting (T_m) temperatures were determined as the midpoint of the change in the slop of the baseline and the maximum of melting peak respectively. These values were determined on the second heating scan since the first scan enable to erase any previous thermal history. The phase crystallinity was determined by eq. (3).

$$X_{DAPA}(\%)=\frac{\Delta H_m-\Delta H_{cc}}{\Delta H_{m0}\times w}\times 100 \quad (3)$$

Where $\Delta H_{m0}=190$ J g^{-1} for 100% crystalline DAPA,[24] w is the DAPA weight percentage in the blend, ΔH_m corresponds to the melting enthalpy, and ΔH_{cc} is the enthalpy of cold crystallization.

A scanning electron microscope (SEM), TESCAN Vegan 3 (Czech Republic), with a 10 kV accelerating voltage was used to examine the dimensions of the fibers, the dispersion of the fibers in the matrix and finally the fiber/matrix affinity. Biocomposite samples were analyzed after cryogenic fracture in liquid nitrogen. All surfaces were gold-coated on a Quorum Technology coater sputter to avoid electric discharges during the analysis.

Uniaxial tensile tests were carried out on an Instron 5585H (United States) apparatus equipped with a load cell of 5 kN. The experiments were performed at room temperature under a constant strain rate of 10^{-2} s^{-1} on samples with dimensions of 20 mm × 4 mm × 1 mm. Young's modulus (E), tensile

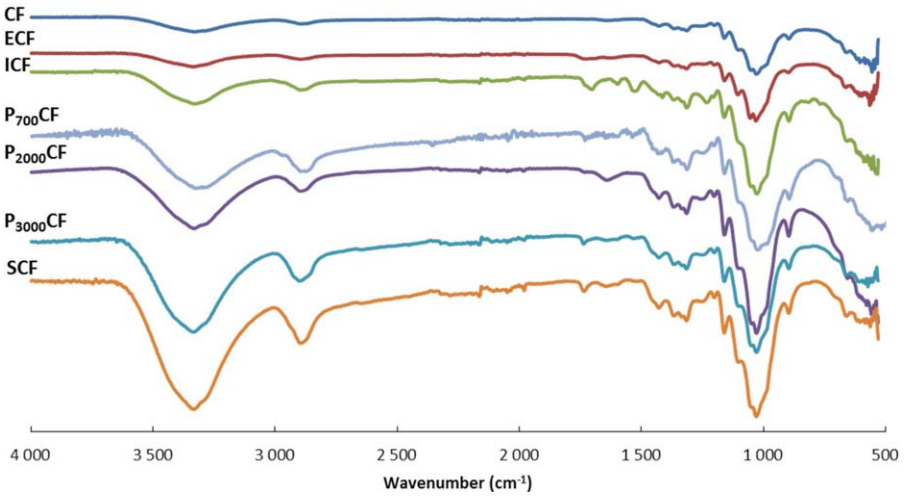

Figure 2. FTIR spectra of neat and modified cellulose fibers. [Color figure can be viewed in the online issue, which is available at wileyonlinelibrary.com.]

strength at break (σ_{max}), and elongation at break (ε_{max}) were determined. The yield point was defined as the maximum of the stress–strain curve before softening.

Dynamic modulus and relaxation temperatures of the composites were measured by a RSA-II apparatus dynamic mechanical analyzer (DMA) from TA instruments, equipped with a liquid-nitrogen cooling system. Experiments were carried out on films in tension/compression mode under a maximum strain ranging from 0.01 to 2% and a frequency of 1 Hz. Samples, with dimensions of 23 mm × 4 mm × 1 mm, were heated from −85 °C to 120 °C at a heating rate of 2 °C min^{-1}.

RESULTS AND DISCUSSION

Characterization of the Different Grafting

FTIR spectra of CF, ECF, ICF, P_{700}CF, P_{2000}CF, P_{3000}CF, and SCF samples are presented in Figure 2 and Supporting Information Figure SI-3. It can be observed that before any modification, CFs displayed characteristic bands[25] corresponding to the OH between 3400 and 3300 cm^{-1}, the C-H vibration from -CH_2 groups at 2894 cm^{-1} and the C—O stretching vibrations of the secondary and primary alcohols at 1103 cm^{-1} and 1051–1029 cm^{-1}, respectively. The esterification of the cellulose with OC is confirmed with the formation of a new peak around 1731 cm^{-1} that corresponds to the C═O stretching vibration of the ester groups.[15] The success of the corresponding chemical treatments is confirmed by FTIR. On the spectra of the ICF sample, we can distinguish the C═O stretching vibration attributed to ester groups and C═O stretching vibration related to the urethane groups at 1730 and 1704 cm^{-1} respectively.[26] The C═C stretching vibration of the aromatic ring at 1597 cm^{-1}, the amide II deformation signal at 1526 cm^{-1} and the C—O—C stretching vibration of the urethane groups[27] at 1233 cm^{-1} are also observed. Characteristic bands assigned to the urethane groups are less visible for P_{700}CF, P_{2000}CF, and P_{3000}CF samples, however a small peak at 1737 cm^{-1} can be observed. On the spectra of the SCF sample, the bands attributed to the Si—O—C groups are hidden by the strong absorption bands of the cellulose.[28] However, at 1645 cm^{-1} the band corresponding to the

Table II. I_{OH} Index Values Measured by Titration and, Experimental Elemental Weight Compositions for Neat and Modified Cellulose Fibers

	%N	%C	%H	I_{OH} (mg KOH g^{-1})
CF	0	43.0	6.2	308 ± 6
ECF	0	46.4	5.9	n.a
ICF	1.0	46.8	6.3	131 ± 2
P_{700}CF	0.2	45.3	6.5	174 ± 2
P_{2000}CF	0	43.0	6.6	229 ± 21
P_{3000}CF	0	45.0	6.4	198 ± 3
SCF	0.3	45.8	6.4	160 ± 2
$C_6H_{10}O_5$ (cellulose)[15]	0	44.5	6.2	n.a.
$C_{14}H_{24}O_6$ (DS = 1)[a]	0	58.3	8.4	n.a.
$C_{23}H_{26}N_2O_8$ (DS = 1)[b]	6.1	60.2	5.7	n.a.

[a] Calculated values considering a degree of substitution (DS) of 1 (one OH per sugar) for the cellulose modified with OC.
[b] Calculated values considering a DS = 1 for the cellulose modified with MMDI and washed with ethanol.

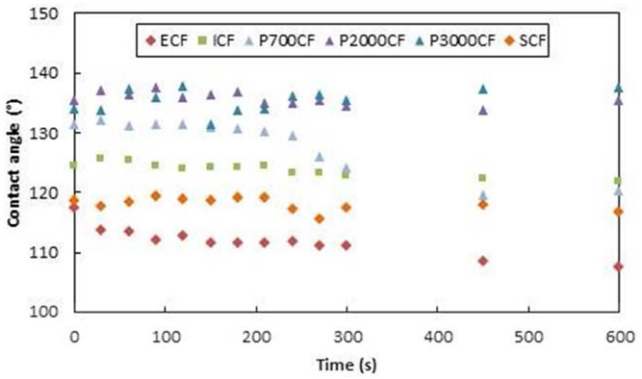

Figure 3. Evolution over time of the contact angle of a drop of water on the surface of cellulose after modification. [Color figure can be viewed in the online issue, which is available at wileyonlinelibrary.com.]

urea group is observed. Urea functions are obtained after the reaction between the amino group of the [*N*-(*n*-Butyl)-3-aminopropyl-trimethoxysilane] and the isocyanate end groups of the prepolymer. The carbonyl band related to the ester groups is also visible at 1737 cm^{-1}.

Finally, these FTIR spectra also demonstrate that all isocyanate groups have disappeared from the reaction mixtures as the 2260 cm^{-1} band (characteristic to the isocyanate functionality) could not be detected.

Results of the elemental analysis for the CF before and after chemical modifications are presented in Table II. The main variations in the values of the elemental compositions were observed for ECF and ICF samples as the corresponding value of DS are about 0.08 and 0.06, respectively.[25] In the P_{700}CF and SCF samples, nitrogen was also detected. The corresponding DS values are below 0.01. For the two other samples, no significant changes in the values of elemental composition before and after modification were observed.

Titration of the hydroxyl functionalities of ICF, P_{700}CF, P_{2000}CF, P_{3000}CF, and SCF samples has also been investigated. The results of which are presented in Table II. The I_{OH} value of neat cellulose is about 308 mg KOH g^{-1}. This value corresponds to the OH which is accessible at the fiber surface and can thus react during the grafting steps. After modification, the residual I_{OH} values decreased (Table II). The corresponding values can be classified as follows: I_{OH} ICF $< I_{OH}$ SCF $< I_{OH}$ P_{700}CF $< I_{OH}$ P_{3000}CF $= I_{OH}$ P_{2000}CF. In the case of the grafting reaction with MMDI, the residual I_{OH} value has been decreased by more than 50%. MMDI, as a very reactive and small molecule compared, for example, to the isocyanate-terminated prepolymers, can easily react with the available OH groups at CF surface. Additionally, above a certain chain length steric hindrance seems to similarly affect the I_{OH} values (P_{700} vs P_{2000} and P_{3000}). Finally, S displays a higher molar mass than P_{700}; however, the obtained I_{OH} values are in the same range. It has been reported[11] that the modification of fibers with isocyanates is more effective than with silanes due to a difference in reactivity. Nevertheless, six methyl siloxane groups are available per prepolymer compared to only two isocyanate groups available in P_{700}. Thus, at the end the reactivities of the two prepolymers (S vs P_{700}) are comparable.

To further characterize the fibers after grafting reactions and to investigate the evolutions of the hydrophobic character of the fiber surfaces, contact angle measurements have been performed (Figure 3). For similar CFs, a contact angle of 47° was previously measured for a cellulose substrate in contact with water.[29] After chemical modification, the measured contact angles ranged from 110 to 140°. The variations of contact angles with time (Figure 3) indicate that ICF and P_{xxx}CF exhibit a higher hydrophobic character than ECF or SCF systems. The gap observed between P_{2000}CF and SCF may be due to the higher amine concentration at the surface of SCF as reported by Bledzki *et al.*[11] The longer the chain of the alcohol grafted on MMDI, the higher the contact angle will be. In agreement with previous results, contact angle measurements show that chemical modifications occurred at CF surface.

Prior to the preparation of the biocomposites, the thermal stability of the modified cellulosic fibers was determined by TGA analyses under air. TGA and DTG curves of neat and modified CF are shown in Figure 4. At the beginning of the analysis, the first weight loss for neat and modified cellulose is attributed to water evaporation. The maximum temperature of this first step degradation is observed at 32 °C for CF, with an increase of more than 10 °C for modified cellulose, in agreement with the chemical modification of the fibers surface. Unmodified cellulose degradation principally occurs in one step after 200 °C. At temperature above 300 °C, cellulose is mainly decomposed in levoglucosan and other anhydroglucose compounds.[30,31] At the end of the analysis (700 °C) no residual char is obtained. Apart from ECF and ICF, modified cellulose display the same

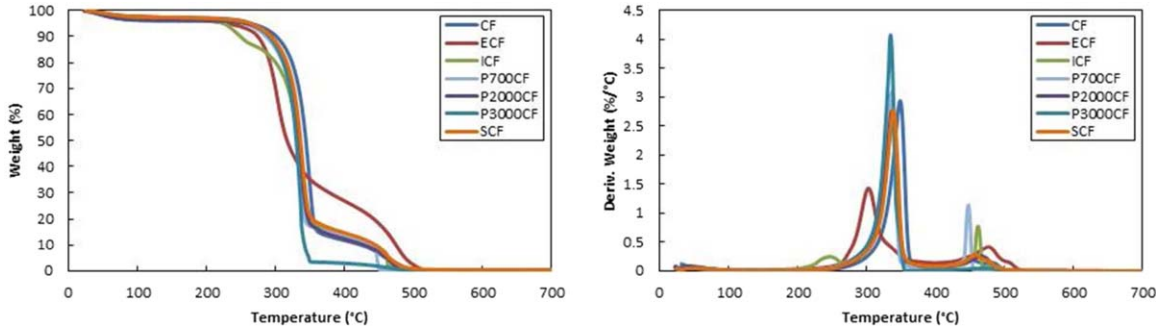

Figure 4. TGA and DTG curves of neat and modified cellulose fibers under air. [Color figure can be viewed in the online issue, which is available at wileyonlinelibrary.com.]

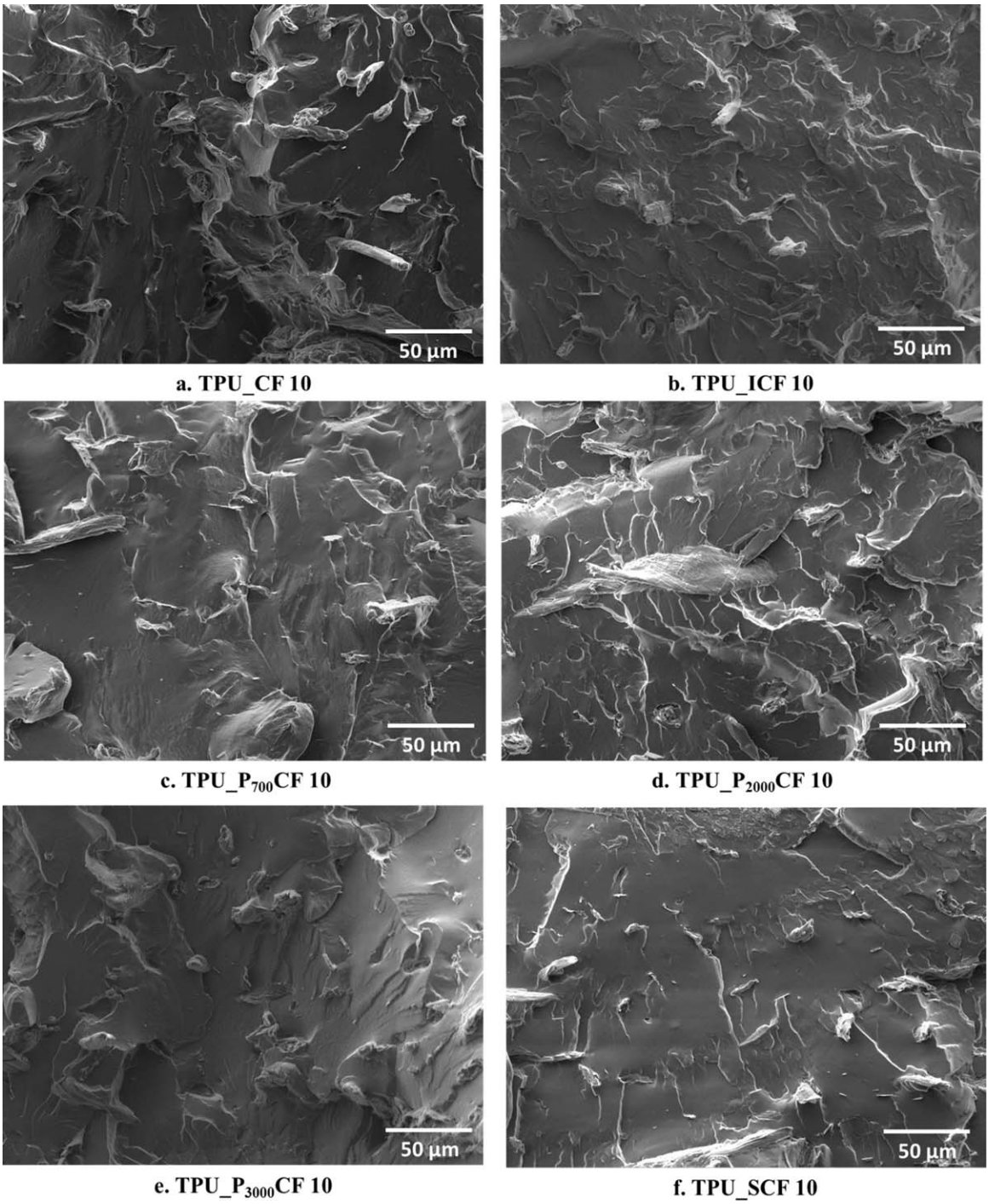

Figure 5. SEM images after cryogenic fracture of TPU composites based on neat or modified cellulose fibers.

degradation steps than neat CF. Both ECF and ICF are less stable as they start to decompose at temperatures significantly lower than 274 °C. This observation was previously reported in the case of cellulose esters,[14,32] and attributed to the decrease in crystallinity at surface associated with the esterification reaction. Moreover, ICF display a three-step degradation. According to literature,[33] the first stage of degradation may be related to the degradation of the urethane bond. However, despite the lower thermal stability of ECF and ICF, all modified cellulosic fibers can be processed at 150 °C to obtain DAPA and/or TPU-based biocomposites, without major degradation.

Analysis of the Biocomposites

Morphology. SEM images of the TPU-based biocomposites obtained after cryogenic fracture are presented in Figure 5. The CFs are well distributed within the matrix but numerous cavities and fibers pulled out can be observed due to rather

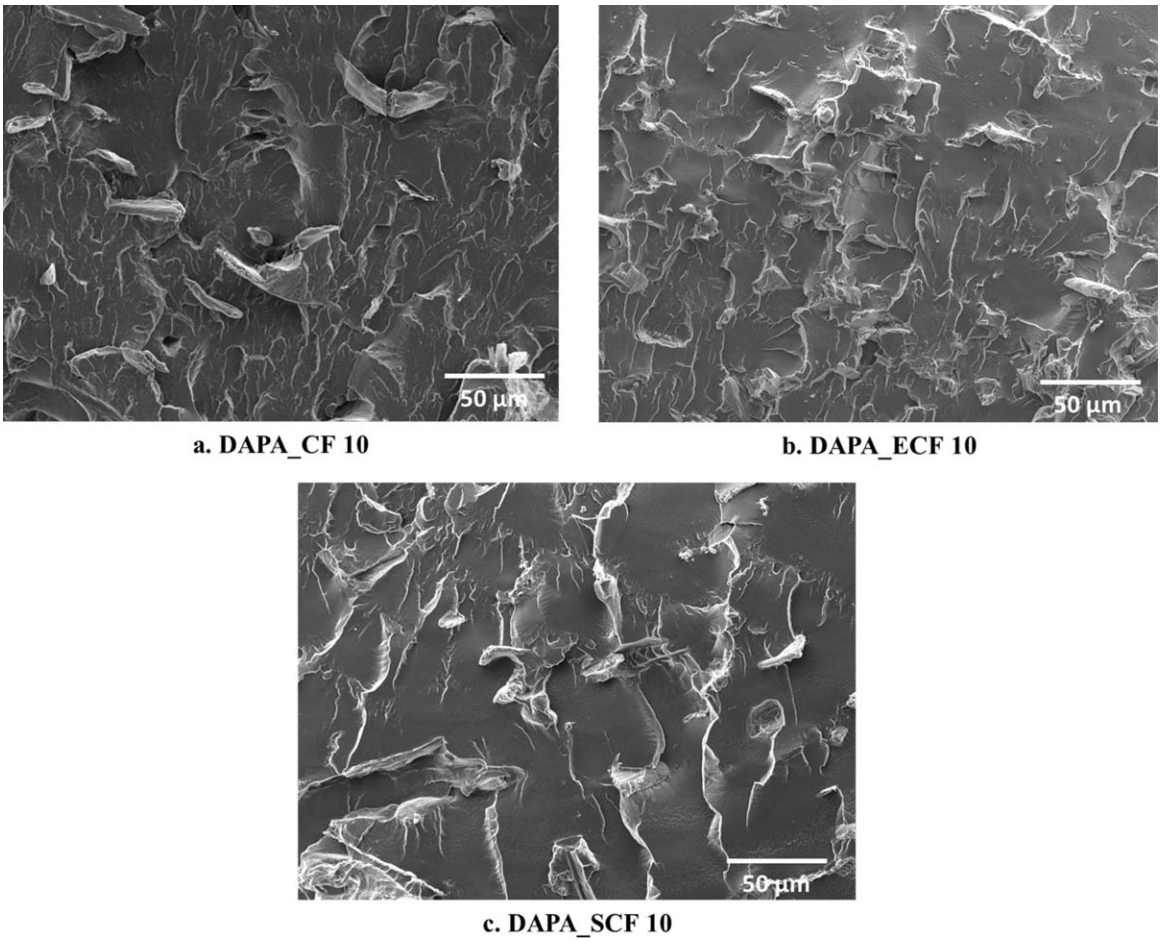

Figure 6. SEM images after a cryogenic fracture of DAPA composites based on neat or modified cellulose fibers.

weak TPU/CF interfacial adhesion. Figure 5(b–f) show fractured surface with modified CF. It can be seen that fibers are still well dispersed within the matrix. In this case, only few holes are noticed and the fibers fractures are mainly located at the sample surface, indicating improved fiber/matrix compatibility.

On Figure 5(b), it is noticeable that the matrix-fiber adhesion was improved after grafting with MMDI. Nevertheless, the wetting of the fibers by the matrix is not complete as some gaps are noticed at interface. With the grafting to approach, fibers appear well embedded into the TPU matrix. In the case of TPU_P_{2000}CF [Figure 5(d)], a coating at the surface of the CF

Table III. Thermal Properties of Neat Polymers, and Biocomposites Based on Neat or Modified Cellulose Fibers

	$T_{g\ TPU}$ (°C)	$T_{g\ DAPA}$ (°C)	$T_{c\ DAPA}$ (°C)	$\Delta H_{c\ DAPA}$ (J g^{-1})	$T_{m\ DAPA}$ (°C)	$\Delta H_{m\ DAPA}$ (J g^{-1})	$T_{cc\ DAPA}$ (°C)	$\Delta H_{cc\ DAPA}$ (J g^{-1})	$X_{c\ DAPA}$ (%)
TPU	−48	—	—	—	—	—	—	—	—
TPU_CF 10	−47	—	—	—	—	—	—	—	—
TPU_ICF 10	−49	—	—	—	—	—	—	—	—
TPU_P_{700}CF 10	−47	—	—	—	—	—	—	—	—
TPU_P_{2000}CF 10	−48	—	—	—	—	—	—	—	—
TPU_P_{3000}CF 10	−49	—	—	—	—	—	—	—	—
TPU_SCF 10	−49	—	—	—	—	—	—	—	—
DAPA	—	6	39	3.9	122	20.4	40	12.7	4.1
DAPA_CF 10	—	4	44	11.2	119	17.4	45	4.9	7.3
DAPA_ECF 10	—	4	45	12.2	120	16.7	45	3.9	7.5
DAPA_SCF 10	—	6	47	12.9	120	18.1	46	3.3	8.6

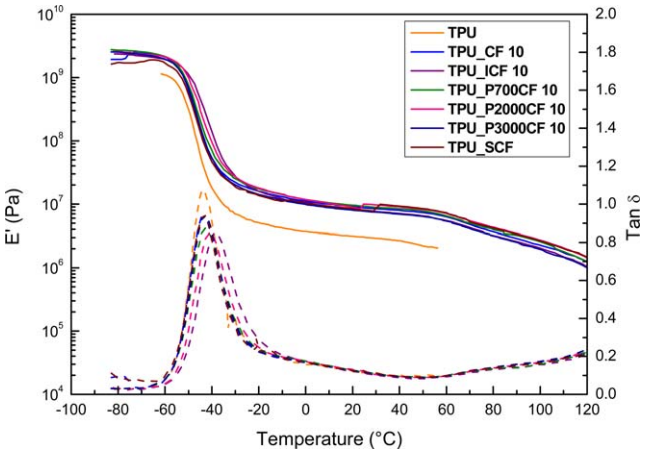

Figure 7. Storage modulus and damping factor versus temperature of TPU and corresponding biocomposites from DMA. [Color figure can be viewed in the online issue, which is available at wileyonlinelibrary.com.]

is clearly visible, indicating a high interfacial adhesion in prefect agreement with previous results. Grafting agents (MMDI, P_{xxx} and S) and the TPU are aromatic and their delocalized π electrons may provide strong interactions by π stacking, leading to an improvement of the interfacial adhesion as previously reported.[11] Hydrogen bonding interactions between the urethane or the amino groups of the grafting agents and the urethane groups present in the HS of the TPU may also increase the quality of the interphase.

The morphologies of DAPA-based composites after SEM observations are reported in Figure 6. As observed previously, CFs are well dispersed within DAPA but cavities and pulled out fibers are identified after cryogenic fracture [Figure 6(a)]. Figures 6(b,c) show that modified CFs are well dispersed within the matrix and no gaps at the interface are detected. In the case of the SCF fibers, hydrogen bonding interactions between the urethane or the amino groups of the grafting agent and the amine groups present in the DAPA may favor the creation of an interphase. Esterified CF appear to be partially destructured by the chemical treatment as, for instance, cellulose fibrils are clearly distinguished (Supporting Information Figure SI-5). This could lead to a higher specific surface.

Thermal and Structural Properties. ATG and DTG thermograms of the different biocomposites are presented in ESI (Supporting Information Figure SI-6). The addition of neat or modified fibers does not impact significantly the thermal degradation of the corresponding biocomposites, as the curves overlay each other. Concerning DSC data, crystallization temperature (T_c), cold crystallization temperature (T_{cc}) corresponding to the crystallization preceding melting, T_g and T_m measured for each matrix and their composites, as well as the corresponding enthalpies (ΔH_c, ΔH_{cc}, and ΔH_m), are presented in Table III. In the case of TPU-based composites, the T_g

Table IV. Storage Modulus, Loss Modulus, Damping Factor and Relaxation Temperatures for Neat Polymers, Blends, and Corresponding Biocomposites with Neat or Modified Cellulose Fibers from DMA

	E′ at 50°C (MPa)	*E″* at 50°C (MPa)	Relaxation temperature (°C)/tan δ value (at maximum peak)[a]	Relaxation temperature (°C)/tan δ value (at maximum peak)[b]
TPU	2.2	0.2	−44/1.07	n.a.
TPU_CF 10	7.3	0.6	−44/0.93	n.a.
TPU_ICF 10	6.6	0.5	−38/0.85	n.a.
TPU_P_{700}CF 10	7.7	0.7	−42/0.88	n.a.
TPU_P_{2000}CF 10	8.3	0.7	−40/0.85	n.a.
TPU_P_{3000}CF 10	6.4	0.6	−42/0.94	n.a.
TPU_SCF 10	6.7	0.6	−44/0.94	n.a.
DAPA	146.1	15.0	n.a.	22/0.19
DAPA_CF 10	245.9	22.6	n.a.	18/0.18
DAPA_ECF 10	165.9	19.7	n.a.	20/0.17
DAPA_SCF 10	185.6	21.6	n.a.	20/0.17
(80/20) Blend	3.7	0.4	−43/0.91	n.a.
(80/20)_CF 10	13.1	1.4	−43/0.82	n.a.
(80/20)_P_{2000}CF 10	10.8	1.1	−41/0.80	n.a.
(80/20)_SCF 10	10.3	1.1	−42/0.82	n.a.
(50/50) Blend	17.7	3.1	−48/0.25	22/0.20
(50/50)_CF 10	47.3	5.9	−48/0.23	23/0.20
(50/50)_P_{2000}CF 10	65.9	7.9	−46/0.23	20/0.19
(50/50)_SCF 10	57.6	5.7	−48/0.25	20/0.17

[a] Related to the TPU phase.
[b] Related to the DAPA phase.

Table V. Young Modulus, Yield Stress, Maximum Stress and Elongation at Break of TPU/DAPA Biocomposites Containing 10 wt % Neat or Modified Cellulose Fibers

	Young Modulus (MPa)	Yield stress (MPa)	Tensile strength (MPa)	Elongation at break (%)
(80/20) Blend	4.4 ± 0.1	2.3 ± 0.2	2.8 ± 0.2	389 ± 95
(80/20)_CF 10	9.9 ± 0.5	3.0 ± 0.2	3.6 ± 0.1	164 ± 16
(80/20)_P_{2000}CF 10	10.7 ± 1.3	3.2 ± 0.1	3.7 ± 0.1	130 ± 32
(80/20)_SCF 10	11.5 ± 0.2	3.0 ± 0.1	3.4 ± 0.1	158 ± 22
(50/50) Blend	45.6 ± 2.6	4.0 ± 0.1	6.8 ± 0.5	460 ± 29
(50/50)_CF 10	52.7 ± 4.7	6.1 ± 0.2	6.9 ± 0.4	321 ± 39
(50/50)_P_{2000}CF 10	60.9 ± 6.7	6.9 ± 0.6	7.3 ± 0.4	221 ± 31
(50/50)_SCF 10	46.2 ± 3.2	5.9 ± 0.3	6.9 ± 0.9	347 ± 85

(related to the SS) is not impacted by the addition of neat or modified CF. Regarding, DAPA-based composites, T_g of the DAPA_10 SCF is slightly shifted toward higher temperatures. The mobility of the DAPA chains is restricted, as hydrogen bonding interactions with SCF occurred, in agreement with SEM observations. Some differences are also noticed for the T_c and the T_{cc} when neat or modified fibers are introduced into DAPA. A shift toward higher values is observed for crystallization temperatures with CF, this indicates that CF act as nucleating agent during the crystallization step. This tendency is also noticed for DAPA_10 ECF and SCF and was already reported by Leszczyńska *et al.* for biocomposites based on PA 4.10 with modified micro-fibrillated cellulose.[34] An increase of the degree of crystallinity of the DAPA phase is also observed when CF, ECF, and SCF are introduced into the matrix. The fibers act as nucleating agent, particularly in the case of SCF. Nucleation of the DAPA phase may easily occur at the interphase between the matrix and the grafting agent.

XRD analyses of DAPA, CF, and DAPA-based composites are presented in the ESI (Supporting Information Figure SI-4). DAPA exhibits a very strong diffraction signal with a maximum at approx. 2θ = 21–21.2° corresponding to distances of approx. 4.2 Å. This distance is characteristic of the average separation between amorphous chains in liquid-like short-range interaction.[35] Additional broad and weak signal are observed at approx. 2θ = 19° and 2θ = 7.1°. CF display three main signals at 2θ = 15.8°, 22.2 and 2θ = 34.5° corresponding to distances of about 5.6, 4.0, and 2.6 Å, characteristic of cellulose I polymorphism.[36] Finally, all the main peaks of DAPA and CF can be identified on the X-ray spectra of the DAPA biocomposites. Only a slight shift toward higher angle values is observed meaning that distances between the amorphous chains of the matrix are reduced. However, these spectra clearly underlines that crystallographic organization of DAPA is not modified with the corresponding biocomposites. Moreover, specific trans-cristallinity at the interface has not been identified.

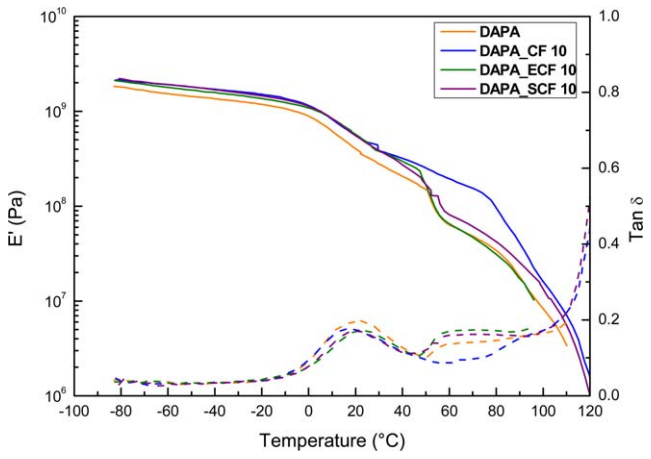

Figure 8. Storage modulus and damping factor versus temperature of DAPA and corresponding biocomposites. [Color figure can be viewed in the online issue, which is available at wileyonlinelibrary.com.]

Thermo-Mechanical Properties. Thermo-mechanical properties of the TPU, DAPA, and TPU/DAPA biocomposites are reported in Figures 7 to 9, Figure 11 and Tables IV and V. In Figure 7 and Supporting Information Figure SI-7, the curve corresponding to the TPU is typical of a thermoplastic elastomer behavior. At low temperatures, TPU properties are governed by SS/HS segregation. From −60 to −20 °C, the storage modulus of the TPU shows a significant decrease, almost 2.5 decades, associated with a maximum of tan δ. This corresponds to the glass-rubber transition and it is followed by a large plateau in the terminal

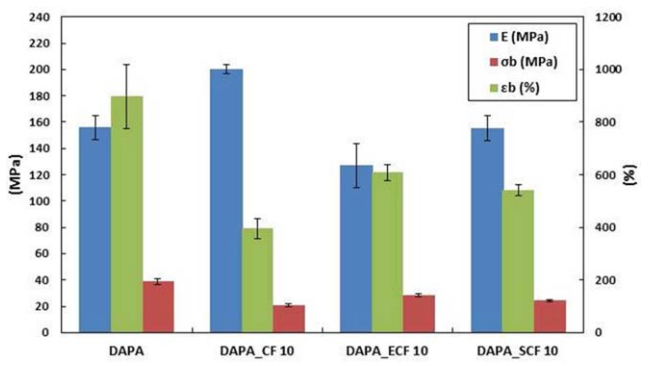

Figure 9. Young modulus, yield stress, maximum stress, and elongation at break of TPU or DAPA biocomposites with neat or modified cellulose fibers, from uniaxial tensile tests. [Color figure can be viewed in the online issue, which is available at wileyonlinelibrary.com.]

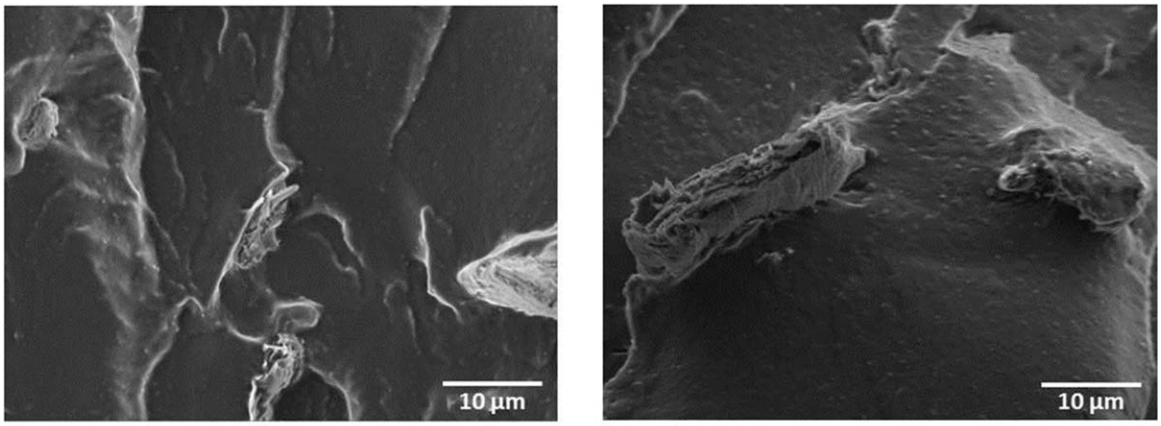

a. TPU/DAPA (80/20)_P_{2000}CF 10 b. TPU/DAPA (80/20)_SCF 10

Figure 10. SEM images after cryogenic fracture of ternary systems: TPU/DAPA 80/20 biocomposites with modified cellulose fibers.

zone. With 10 wt % of CF, the storage modulus (E') is improved over the whole range of temperature. For instance, values summarized in Table IV show that E' at 50 °C is increased 3.3 times, to 7.3 MPa. A similar trend is observed for the Young's modulus from uniaxial tensile tests at room temperature (Figure 9). Meanwhile, tensile strength dropped showing that load transfer between the matrix and the neat fibers is low. This is connected with the weak interfacial adhesion observed, for example, in Figure 5(a). An increase in stiffness also dramatically affects the elongation at break (ε_b). The ε_b of the TPU is about 900% and drops to almost 300% when CF are introduced (Figure 9 and Table V).

With 10 wt % of modified cellulose into the TPU, higher E' values at 50 °C are reached, TPU_P_{700}CF 10 and TPU_P_{2000}CF 10 systems display a value of 7.7 and 8.3 MPa, respectively. At room temperature, the stiffness is also improved as the Young's modulus is increased by 25% with P_{2000}CF, compared to CF. Moreover, for the same level of elongation at break, TPU-based composites with modified CFs are stiffer than with neat CF.[37] These observations can be correlated with the decrease of the damping factor at the maximum peak observed for TPU_ICF, TPU_P_{2000}CF, and TPU_P_{700}CF in Figure 7 and Table IV. Indeed, this drop expresses the ability of the biocomposite to absorb energy. The load transfer is also improved under mechanical manipulations due to higher interfacial adhesion.

Finally, improvement of the interfacial adhesion can also be demonstrated through the analysis of the tan δ curve (Figure 7). Relaxation temperature (T_α) reported in Table IV for TPU and TPU-based composites can be associated with the mobility of SS from TPU. T_α moved toward higher temperatures with ICFs and P_{2000}CFs due to a decrease of the macromolecular motions,[6,38] via hydrogen bond and/or π stacking interactions. Chemical modifications, particularly with MMDI and P_{2000}, favor matrix/fibers interactions as previously shown, for example, on Figure 5(d).

DAPA display a typical behavior of semi-crystalline thermoplastics (Figure 8). From DMA or uniaxial tensile tests, most of the major improvements related to the mechanical properties of DAPA systems are observed for biocomposites based on CF (Figures 8 and 9 and Table IV). In Figure 8, the increase of the stiffness (E') over the whole temperature range can be both attributed to the higher degree of crystallinity of the matrix (reported by DSC analyses) and to the addition of fibers. In the same way, DAPA_CF 10 also displays a 30%-increase of the Young's modulus at room temperature (Figure 9).[2] According to Figure 8, grafting with SCF and ECF show an improvement in the storage modulus up to the transition of relaxation α. In the case of ECF, it can be linked to the generation of microfibrils. Beyond the α transition the DAPA matrix starts to flow and the storage modulus values of DAPA_ECF and SCF biocomposites reach those of neat DAPA. Furthermore, regarding tan δ curves (Figure 8), T_α is not impacted by the chemical modification of the fibers. Thus, modified fiber/matrix interactions through hydrogen bonds are not sufficient enough to modify the mobility of the DAPA chains.

CF, P_{2000}CF, and SCF were also introduced in TPU/DAPA (80/20) and (50/50) blends, respectively to obtain ternary systems. In a previous study, we described the corresponding morphology of the 80/20 and 50/50 blends.[5] Eighty/twenty blends show

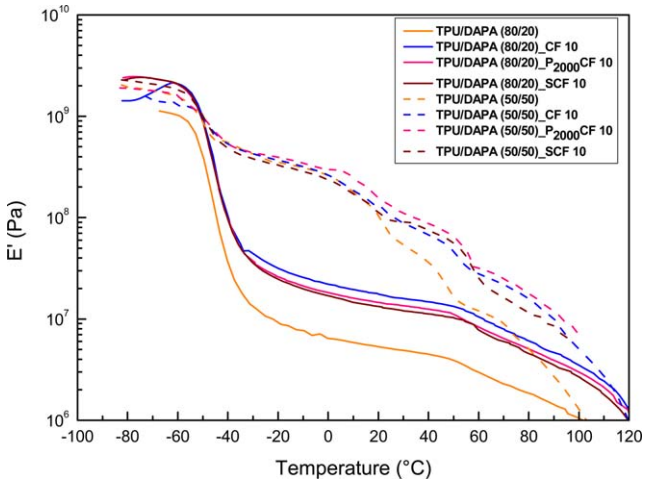

Figure 11. Storage modulus versus temperature of TPU/DAPA blends and corresponding biocomposites. [Color figure can be viewed in the online issue, which is available at wileyonlinelibrary.com.]

a disperse morphology since DAPA was homogeneously dispersed in TPU matrix, as a micron-sized granular phase.[4,5] Fifty/Fifty blends present a co-continuous morphology. SEM observations of the 80/20 biocomposites with P_{2000}CF and SCF are presented in Figure 10. A granular phase associated to the DAPA is still observed showing that the addition of modified fibers does not disturbed the pre-existing blend morphology. Nevertheless, the decrease of the TPU content, with addition of DAPA can lower the intensities of the corresponding transitions and then interactions cannot be easily detected.

Ensuing DMA results and uniaxial tensile properties are reported in Tables IV and V, respectively. Focusing on Figure 11 which shows the storage modulus versus the temperature, we notice that the CFs in 80/20 systems considerably increases E' values in the studied temperature range. For instance, at 50 °C the storage modulus raises from 3.7 to 13.1 MPa (3.5 times). However, this rise is not impacted by the chemical modifications. The same trend is observed with uniaxial tensile testing (Table V). Regarding 50/50 biocomposites, the addition of CF limits the drop in the storage modulus which results in a higher thermal-mechanical stability of the material at high temperature.[3] Chemical modifications, particularly with $P_{2000,}$ lead to higher mechanical properties (after the α-transition associated to the SS of the TPU). Among the different ternary (50/50) systems, (50/50)_P_{2000}CF exhibits the highest Young's modulus. Additionally, this latter system displays a higher tensile strength pointing out good interfacial adhesion and interactions. The slight shift of T_α (TPU) toward higher temperatures shown in Table V for this system corroborates the existing interactions (π, H-bonds) within the TPU phase.

CONCLUSIONS

In this study, we have developed advanced biocomposites based on binary or ternary systems with thermoplastic matrices (TPU and DAPA) and modified or neat CF. CF were specifically modified either to establish high interfacial adhesion and compatibility with TPU or DAPA. From the three grafting approaches tested (Figure 1), the best performing were the isocyanate-terminated prepolymer P_{2000} and the silane-terminated prepolymer (S) modifications. Due to some chemical similarities with the matrices, these two grafting agents were able to easily interact with TPU or DAPA, through π-stacking or hydrogen bonds. The storage modulus (DMA) and the Young's modulus (uniaxial tensile test) were improved at least three times in the case of TPU_P_{2000}CF biocomposite. Improvement of the interfacial adhesion and mechanical properties was also observed in the case of the ternary biocomposites and more especially for the 50/50 TPU/DAPA reinforced system with P_{2000}CF as, for instance, the storage modulus at 50 °C was augmented 1.4 times. In the case of the 80/20 TPU/DAPA reinforced systems, the granular phase associated with DAPA is still observed showing that the addition of modified fibers does not disturb the pre-existing blend morphology.

These fully sustainable composites are able to compete with petroleum-based systems currently in the use, for instance, in the building or in the automotive sector. Additional investigations must be conducted to test the degradation of these materials for long term applications and to fulfill the corresponding requirements. Moreover, lingo-cellulosic fillers must also be tested as they provide a lower cost alternative the CF.

ACKNOWLEDGMENTS

The authors thank J. Rettenmaier and Söhne for the cellulose sample, Oleon, Croda, and Repsol for polyol samples and Evonik for the amino-silane samples. They are also grateful to Bpi-France and ANRT for their financial supports and to Stéphanie Laurichesse and Alexandru Sarbu from Soprema, for helpful discussions.

REFERENCES

1. Avérous, L.; Le Digabel, F. *Carbohydr. Polym.* **2006**, *66*, 480.
2. Hablot, E.; Matadi, R.; Ahzi, S.; Avérous, L. *Compos. Sci. Technol.* **2010**, *70*, 504.
3. Hablot, E.; Matadi, R.; Ahzi, S.; Vaudemond, R.; Ruch, D.; Avérous, L. *Compos. Sci. Technol.* **2010**, *70*, 525.
4. Reulier, M.; Avérous, L. *Eur. Polym. J.* **2015**, *67*, 418.
5. Reulier, M.; Matadi Boumbimba, R.; Rasselet, D.; Avérous, L. *J. Appl. Polym. Sci.* **2016**, *133*, DOI: 10.1002/app.43055.
6. Ly, B.; Thielemans, W.; Dufresne, A.; Chaussy, D.; Belgacem, M. N. *Compos. Sci. Technol.* **2008**, *68*, 3193.
7. Amash, A.; Zugenmaier, P. *Polymer* **2000**, *41*, 1589.
8. Pasquini, D.; Teixeira, E. d. M.; Curvelo, A. A. d. S.; Belgacem, M. N.; Dufresne, A. *Compos. Sci. Technol.* **2008**, *68*, 193.
9. Feldmann, M.; Bledzki, A. K. *Compos. Sci. Technol.* **2014**, *100*, 113.
10. Bledzki, A. K.; Gassan, J. *Prog. Polym. Sci.* **1999**, *24*, 221.
11. Bledzki, A. K.; Reihmane, S.; Gassan, J. *J. Appl. Polym. Sci.* **1996**, *59*, 1329.
12. Vaca-Garcia, C.; Borredon, M. E. *Bioresour. Technol.* **1999**, *70*, 135.
13. Vaca-Garcia, C.; Gozzelino, G.; Glasser, W. G.; Borredon, M. E. *J. Polym. Sci. Part B: Polym. Phys.* **2003**, *41*, 281.
14. Freire, C. S. R.; Silvestre, A. J. D.; Neto, C. P.; Belgacem, M. N.; Gandini, A. *J. Appl. Polym. Sci.* **2006**, *100*, 1093.
15. Pasquini, D.; Belgacem, M. N.; Gandini, A.; Curvelo, A. A. d. S. *J. Colloid Interface Sci.* **2006**, *295*, 79.
16. Trejo-O'Reilly, J. A.; Cavaille, J. Y.; Gandini, A. *Cellulose* **1997**, *4*, 305.
17. Priya, B.; Singha, A. S.; Pathania, D. *Polym. Eng. and Sci.* **2015**, *55*, 474.
18. Singha, A. S.; Thakur, B. P.; Pathania, D. *Int. J. of Polym. Anal. and Ch.* **2014**, *19*, 115.
19. Bueno-Ferrer, C.; Hablot, E.; Perrin-Sarazin, F.; Garrigós, M. C.; Jiménez, A.; Avérous, L. *Macromol. Mater. Eng.* **2012**, *297*, 777.
20. Thiebaud, S.; Borredon, M. E. *Bioresour. Technol.* **1995**, *52*, 169.

21. Thiebaud, S.; Borredon, M. E.; Baziard, G.; Senocq, F. *Bioresour. Technol.* **1997**, *59*, 103.
22. Laurichesse, S.; Huillet, C.; Averous, L. *Green Chem.* **2014**, *16*, 3958.
23. Benyahya, S.; Aouf, C.; Caillol, S.; Boutevin, B.; Pascault, J. P.; Fulcrand, H. *Ind. Crops Prod.* **2014**, *53*, 296.
24. Van Krevelen, D. W. Properties of Polymers: Their Correlation with Chemical Structure; Their Numerical Estimation and Prediction from Additive Group Contributions, Third Completely Revised Edition; Elsevier, **1997**.
25. Siqueira, G.; Bras, J.; Dufresne, A. *Langmuir* **2009**, *26*, 402.
26. Irusta, L.; Fernandez-Berridi, M. J. *Polymer* **2000**, *41*, 3297.
27. Wilhelm, C.; Gardette, J. L. *Polymer* **1997**, *38*, 4019.
28. Abdelmouleh, M.; Boufi, S.; Belgacem, M. N.; Duarte, A. P.; Ben Salah, A.; Gandini, A. *Int. J. of Adhes. and Adhes.* **2004**, *24*, 43.
29. Le Digabel, F.; Boquillon, N.; Dole, P.; Monties, B.; Averous, L. *J. Appl. Polym. Sci.* **2004**, *93*, 428.
30. Ranzi, E.; Cuoci, A.; Faravelli, T.; Frassoldati, A.; Migliavacca, G.; Pierucci, S.; Sommariva, S. *Energy Fuels* **2008**, *22*, 4292.
31. Shafizadeh, F. *J. Anal. Appl. Pyrolysis* **1982**, *3*, 283.
32. Jandura, P.; Riedl, B.; Kokta, B. V. *Polym. Degrad. Stabil.* **2000**, *70*, 387.
33. Gironès, J.; Pimenta, M. T. B.; Vilaseca, F.; de Carvalho, A. J. F.; Mutjé, P.; Curvelo, A. A. S. *Carbohydr. Polym.* **2007**, *68*, 537.
34. Leszczyńska, A.; Kiciliński, P.; Pielichowski, K. *Cellulose* **2015**, 1.
35. Hablot, E.; Donnio, B.; Bouquey, M.; Avérous, L. *Polymer* **2010**, *51*, 5895.
36. O'Sullivan, A. C. *Cellulose* **1997**, *4*, 173.
37. Saheb, D. N.; Jog, J. P. *Adv. Polym. Technol.* **1999**, *18*, 351.
38. Bergeret, A.; Bozec, M. P.; Quantin, J. C.; Crespy, A.; Gasca, J. P.; Arpin, M. *Polym. Compos.* **2004**, *25*, 12.